Tassi, Pablo; Villaret, Catherine; Hervouet, Jean-Michel

New developments and validations for the 3D sediment transport modelling within the Telemac Modelling System

New developments and validations for the 3D sediment transport modelling within the Telemac Modelling System

Pablo TASSI
EDF R&D – Laboratoire National d'Hydraulique et Environnement (LNHE)
Chatou, France
pablo.tassi@edf.fr

Catherine VILLARET & Jean-Michel HERVOUET
EDF R&D – Laboratoire National d'Hydraulique et Environnement (LNHE)
Saint Venant Laboratory for Hydraulics
Chatou, France

Abstract— In this work, some recent developments for the 3D sediment transport modelling are presented in the framework of the Telemac Modelling System. The mathematical formulation of the implemented modules is discussed and some special issues arising from the treatment of the bottom boundary are addressed. In particular, the choice of the near-bed concentration and reference level is analyzed and a new methodology is introduced to avoid infinite concentrations at the bed level, while conservation properties are upholding. The model is verified by comparison with the well-known analytical solution of Rouse and validated with 2D simulations and experimental data from the trench evolution setup of van Rijn. The sensitivity to the sediment parameterizations and turbulence closure relationships is also analyzed. In all cases, the 3D model performs well when compared against analytical results and measurements of velocity and suspended sediment profiles, and shows good agreement in reproducing changes of the bed.

I. INTRODUCTION

Over the years, two-dimensional (2D), depth-averaged numerical models have been developed to predict sediment transport rates and changes of bed level [15]. The 2D approach, strictly valid under well established hypothesis, has been widely used by the engineering community to compute medium to long term bed evolution in large-scale applications. However, situations where strong secondary flows, stratification effects or complicated spiral motions are present can only be represented realistically by three-dimensional (3D) models. Furthermore, detailed 3D modelling of flow and suspended sediment transport can provide useful information on the complex flow structures characterized by strong vertical gradients of both velocity and suspended sediment concentration in the near-bed boundary layer [4].

Despite some recent progress in the development of full 3D models, see for example [1, 8, 14, 16] and references therein, some relevant issues such as the inherent difficulty to capture the vertical flow structure, the dependence of model results to the bottom boundary conditions and the choice of turbulence closures has not been yet emphasized enough. In this work, we address some of these issues by comparing 2D and 3D numerical simulations of coupled flow and suspended sediment transport on the basis of the open-source Telemac Modelling System [11].

In the 2D model, the depth-averaged suspended sediment concentration is calculated by solving an advection-diffusion equation. In this 2D transport equation, a correction factor can be applied to the advection term in order to account for the non-uniform vertical distribution of flow velocity and concentration over the depth [7]. In the 3D model, the flow field is computed by solving the continuity equation and the Reynolds-averaged Navier-Stokes equations. The Reynolds stress tensor is modelled by suitable turbulence closure relationships. The suspended sediment load is then calculated by solving the full 3D convection-diffusion equation for the suspended sediment concentration distribution. As pointed by Begnudelli *et al*. [2], sediment transport rate predictions can be highly sensitive to the choice of the near-bed concentration and reference level. Therefore, a methodology is proposed to avoid infinite concentrations at the bed level, while conservation properties are upholding.

The capabilities of both 2D and 3D models are demonstrated by comparing numerical results against analytical solutions and experimental data. First, we perform numerical simulations in steady, uniform flows for a prescribed flow rate and variable bed roughness. The 3D model results are validated against classical turbulent boundary layer concepts, like the logarithmic velocity profile and the Rouse distribution of concentration. The very large gradients of velocity and sediment concentration within the near-bed boundary layer are accurately captured by using a suitable refined vertical grid. Then, both 2D and 3D models are applied to simulate the laboratory experiment of a migrating trench [12]. The experience of a migrating trench

in a flume is used to validate and compare the 2D and 3D numerical results of velocity profiles, concentration distribution and bed deformation. This reference test has been selected as a validation test by various authors using 2D and 3D numerical models, see *e.g.* [1, 8, 14].

This paper is organized as follows. In Section 2 the 2D and 3D model equations are presented for flow and suspended sediment transport. In Section 3, the computational framework for the solution of the 2D and 3D models is briefly introduced and some important issues arising from the implementation of the 3D sediment transport model are discussed. In Section 4, the 3D model is first verified with the analytical solution of the uniform flow and sediment transport in a steady, uniform channel and the results are compared with the classical and corrected 2D model. Then the model is validated with the experimental setup of van Rijn [12]. Finally, the conclusions and outlook of the work are presented in Section 5.

II. MATHEMATICAL FORMULATION

In this section, we briefly describe the 2D and 3D models for flow and sediment transport.

A. *Three-dimensional hydrodynamic model*

In this work, the 3D flow field is determined by solving the continuity and Reynolds-averaged Navier-Stokes equations in the Cartesian coordinate system:

$$\begin{cases} \dfrac{\partial u_i}{\partial x_i} = 0 \\ \dfrac{\partial u_i}{\partial t} + \dfrac{\partial u_i u_j}{\partial x_j} = F_i - \dfrac{1}{\rho}\dfrac{\partial p}{\partial x_i} + \dfrac{1}{\rho}\dfrac{\partial \tau_{ij}}{\partial x_j} \end{cases} \tag{1}$$

where the summation convention for repeated indices is used. Above, let $x_i = (x_1,x_2,x_3) = (x,y,z)$ denote the spatial coordinates; $t \geq 0$ the time; $u_i = (u_1,u_2,u_3) = (u,v,w)$ the local time-averaged components of the flow velocity, F_i the components of external forces, such as gravity, Coriolis force, etc.; p the mean pressure; ρ the fluid density and τ_{ij} the components of the stress tensor calculated with the Boussinesq hypothesis and related to the gradients of the velocity and the turbulence eddy viscosity ν_t. In this work, two turbulence closure models are used to compute ν_t, namely the mixing length and the standard k–ε turbulence models, see *e.g.* [9, 10].

The continuity and Reynolds-averaged Navier-Stokes equations (1) are completed with initial and boundary conditions. At the inlet boundary, the uniform or the classical rough wall logarithmic profiles can be applied:

$$u(z) = \frac{u_*}{\kappa}\log\frac{z}{z_0} \tag{2}$$

where z is the vertical distance from the theoretical bed level, u_* is the shear velocity, related to the bed shear stress by $u_* = \sqrt{\tau_b/\rho}$, κ is the von Karman constant (≈ 0.40), $z_0 = k_s/30$ is a length scale related to the bottom roughness and k_s the Nikuradse's equivalent bed roughness. A sketch of the theoretical distribution of $u(z)$ is given in Figure 1.

At the outlet boundary, the normal derivatives of the flow variables are set to zero. At the sidewalls, the velocity tangential and normal to the boundary are set to zero (no-slip condition). Finally, the position of the water surface is determined from the solution of the depth-averaged shallow-water continuity equation, see [6]. The input boundary conditions for the k–ε model are taken from [3]:

$$k_{in}(z) = \frac{u_*^2}{\sqrt{c_\mu}}\left(1-\frac{z}{h}\right), \qquad \varepsilon_{in}(z) = \frac{u_*^3(1-z/h)}{\kappa(z+z_0)} \tag{3}$$

with h the water depth and $c_\mu = 0.09$ a coefficient. The eddy viscosity ν_t is related to k and ε by

$$\nu_t = c_\mu \frac{k^2}{\varepsilon} \tag{4}$$

B. *Two-dimensional hydrodynamic model*

To obtain the 2D, depth-averaged, horizontal shallow water equations, the continuity and Reynolds-averaged Navier-Stokes equations (1) are integrated over the depth h using the Leibniz' integral rule, replacing the mean pressure p by the hydrostatic pressure and adopting a movable free surface level $k_s = h + z_b$, with z_b a smooth function representing the bottom level, eventually resulting in:

$$\begin{cases} \dfrac{\partial h}{\partial t} + \dfrac{\partial hU_j}{\partial x_j} = 0 \\ \dfrac{\partial U_i}{\partial t} + \dfrac{\partial hU_iU_j}{\partial x_j} = -gh\dfrac{\partial z_s}{\partial x_i} + \dfrac{1}{\rho}\dfrac{\partial hT_{ij}}{\partial x_j} - \dfrac{1}{\rho}\tau_{b_i} \end{cases} \tag{5}$$

where $U_i = (U_1,U_2)$ are the components of the depth-averaged flow velocity in two space dimensions; g denotes the gravitational acceleration; the bottom shear stress τ_b can be modelled by the well-known quadratic friction law $\tau_{b_i} = C_f \rho |U| U_i$, with $|U| = \sqrt{U_iU_i}$ the Euclidean norm of the horizontal velocity vector and C_f the friction coefficient determined as function of equivalent bed roughness k_s. In this work, the stresses at the free surface are not considered.

The components of the tensor $T_{ij}(i,j = 1,2 = x,y)$, accounting for the depth-averaged normal and horizontal shear stresses, are related to the gradients of the depth-averaged velocities assuming a constant horizontal diffusion coefficient. Details of the full derivation of the shallow water equations, as well as different boundary conditions for different flow regimes can be found in [13].

C. *Three-dimensional suspended sediment transport model*

The suspended sediment load is calculated by solving the full 3D advection-diffusion equation for the suspended sediment concentration distribution, expressed as

$$\frac{\partial c}{\partial t} + \frac{\partial u_j c}{\partial x_j} - w_s\frac{\partial c}{\partial x_3} = \frac{\partial}{\partial x_j}\left(\frac{\nu_t}{\sigma_c}\frac{\partial c}{\partial x_j}\right) \tag{6}$$

with $c = c(x_i,t)$ the suspended sediment concentration, $w_s > 0$ the vertical-settling sediment velocity and σ_c the turbulent Schmidt number, assumed here to be one. The advection-diffusion equation (6) is completed with initial conditions specifying $c(t = 0)$ and boundary conditions as follows.

At the inlet boundary, a local equilibrium concentration profile can be specified. This profile can be derived from equation (6) by assuming uniform and steady flow conditions. If a parabolic distribution of turbulent eddy diffusivity coefficient is adopted, then the vertical distribution of suspended sediment concentration is the classical Rouse profile:

$$\frac{c}{c_{ref}} = \left(\frac{h/z - 1}{h/z_{ref} - 1} \right)^{w_s/\kappa u_*} \tag{7}$$

where c_{ref} and z_{ref} are the equilibrium near-bed concentration and reference level, respectively. In this work, numerical results are performed by using either the formula of van Rijn [12] or the Zyserman and Fredsoe [17] for the reference concentration and associated reference level, where c_{ref} is a function of the local skin friction. The Rouse number $w_s / \kappa u_*$ evidences the effect of gravity against the turbulent diffusion. Equation (7) clearly shows that the concentration is equal to zero at the free surface and can be infinitely large as the distance z tends to zero as the turbulence vanishes. This particular issue is discussed in more detail in Section 3.

At the outlet, the normal gradients of the concentration are set equal to zero. A similar boundary condition can be specified at the sidewalls of the model. At the free surface, the net vertical sediment flux is set to zero, thus:

$$\left(\nu_t \frac{\partial c}{\partial z} + w_s c \right)_{z=z_s} = 0$$

At the bottom, a Neumann type boundary condition is specified, in which the total vertical flux equals the net sediment transport:

$$\left(\nu_t \frac{\partial c}{\partial z} + w_s c \right)_{z=z_{ref}} = D - E$$

The deposition D and entrainment E fluxes can be expressed as $E = w_s c_{z=z_b}$ and $E = w_s c_{ref}$, respectively [5]. To compute the deposition rate D, the concentration at the bed level $z = z_0$ must be determined, as described in Section 3.

D. Two-dimensional suspended sediment transport model

Integrating Eq. (6) over the depth, the 2D depth-averaged horizontal suspended sediment transport model is obtained:

$$\frac{\partial C}{\partial t} + \frac{\partial U_{conv,j} C}{\partial x_j} = \frac{\partial}{\partial x_j} \left(\nu_t \frac{\partial C}{\partial x_j} \right) + \frac{E - D}{h} \tag{8}$$

where C is the depth-averaged suspended-load concentration and $U_{conv,j}$ are the corrected convective velo-cities accounting for the effects of the heterogeneous vertical distribution of suspended sediment, as defined in [7]. In (8) it is assumed that $z_{ref} << h$.

E. Bed evolution

By considering only suspended-load sediment transport, the bed evolution is function of the net sediment flux near the bed given by:

$$(1 - p') \frac{\partial z_b}{\partial t} = D - E \tag{9}$$

where z_b is the position of the bed above datum and $p' \approx 0.40$ is the bed porosity. Once the flow variables are determined by solving the hydrodynamics and suspended sediment transport equations (for 3D or 2D models), changes of bed level are computed from (9) for the cell coincident to the bed, calculating at each time step the net sediment flux $D - E$. Further details on the derivation of the mass balance equation (9) and coupling strategies can be found in [15].

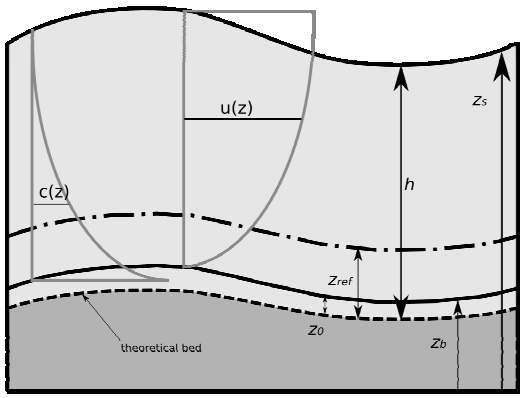

Figure 1. Schematic view of the model variables.

III. NUMERICAL IMPLEMENTATIONS

In this section, some important issues arising from the implementation of the 3D sediment transport model are addressed. For the 2D sediment computations, the reader is referred to the Sisyphe documentation [11].

A. Telemac finite element system

The computational framework for the implementation of the different models is the Telemac Modelling System [11]. This is an open-source, sequential and parallel free-surface solver based on the finite volume and finite element methods. Details of the numerical formulations for the models are given in [6] and not repeated here.

For the 3D model, the domain composed of prismatic elements is built from an unstructured triangulation of the 2D domain, then repeated along the vertical in superimposed layers from the bottom to the free surface. The largest concentration gradients in the model are expected to occur close to the bottom surface. This is where the highest vertical resolution is required and the performance of the numerical model is significantly diminished. Therefore, simulations are performed here with a number of layers vertically distributed with a geometric progression.

B. Bottom boundary layer model

The treatment of the near bed boundary layer in the 3D model is particularly important for sediment transport, which strongly depends on an accurate determination of the bed shear stress and the friction velocity.

According to classical boundary layer concepts, the turbulent eddy viscosity coefficient is proportional to the theoretical (mean) bed level, located at some intermediate point. The vertical balance between the gravity term due to settling and turbulent diffusion no longer holds at the bed level, where the turbulence vanishes, giving rise to infinite concentrations.

In the hydrodynamic model, the mesh is shifted in the vertical direction by a fixed value $z = z_0$ (see Figure 1) relative to the theoretical bed position. The bed origin in the model therefore corresponds to the origin of the velocity profile. This numerical artefact avoids the problem of infinite concentration at the bed. The vertical grid is then refined such that the first grid elevation scales with the bed roughness (of the order of few millimetres) and the consecutive layers follow a geometric progression in the vertical direction, increasing the vertical resolution from the bottom to the top. A detail of the mesh with a geometric progression in the vertical direction is showed in Figure 3.

C. Sediment boundary conditions

The erosion flux E is calculated as an explicit function of the reference concentration at $z = z_{ref}$. The deposition flux D is calculated as an implicit function of the concentration at the (model) bed level ($z = z_0$). In most practical applications, the reference level z_{ref} is generally greater than z_0. The value of the concentration at $z = z_0$ is then obtained by extrapolating the reference concentration from the reference level $z = z_{ref}$ to the model bed level $z = z_0$ (Figure 1), assuming an exponential concentration profile which is consistent with the linear diffusion coefficient:

$$c(z = z_0) \approx c_{ref} \left(\frac{z_{ref}}{z_0} \right)^{w_s / \kappa u_*} \qquad (10)$$

IV. Numerical Examples

In this section, the 3D model results are first compared with the well-known logarithmic velocity and sediment concentration Rouse profiles and validated with the trench migration experience of van Rijn [12].

A. Fully developed uniform steady flow

Both 2D and 3D models are first applied to the simple test case of a fully developed uniform steady flow over a flat bed. Model results can be validated against the classical analytical solution of the Rouse concentration profile and logarithmic velocity profile (which are strictly valid up to the free surface assuming a parabolic distribution for the turbulent eddy viscosity). The main objective of this test is to validate the 3D model resolution, such as number of planes, etc., as well as to test the consistency between the 2D and 3D approach: both models are expected to give the same integrated results in this simple configuration as stated in the introduction, regarding the value of friction velocity, suspended load transport rate and mean depth-averaged concentration. For this test, a flow rate $Q = hu = 0.22\ m^3 s^{-1}$ and a water depth $h = 0.40\ m$ are specified at the channel inlet and outlet, respectively. The computations are performed with the reference concentration formula of Zyserman and Fredsoe [20], with $d_{50} = 0.16\ mm$, $k_s = 2.5\ cm$ and $w_s = 1.50\ cm.s^{-1}$.

In both 2D and 3D models, the reference concentration is calculated as function of skin friction and applied at the reference level ($z_{ref} = 3d_{50}$). Results of shear velocity u_*, depth-averaged concentration C and solid discharge Q_s at the channel outlet are summarized in Table 1. For the 3D model, the values of the depth-averaged concentration are obtained by integrating the concentration $c(z)$ over the water depth.

The effect of the vertical mesh resolution for 6, 12 and 18 layers is presented in Figure 2 for the velocity and concentration profiles. As expected, increasing the number of layers shows convergence to steady profiles. It can also be shown that the gradients of velocity and concentration can be well captured with a reasonable number of layers in the vertical direction.

TABLE I. Uniform steady flow: 2D and 3D results

Model	Type	u_* ($cm.s^{-1}$)	c or C (gl^{-1})	Q_s ($m^2 s^{-1}$)
3D	30 layers	3.87	0.268	1.16×10^{-5}
2D	"classical"	3.87	0.231	1.74×10^{-5}
	"corrected"	3.87	0.231	1.31×10^{-5}

B. Flow in a migrating trench

The laboratory experiment, conducted by van Rijn [12], was performed in a straight channel at Delft Hydraulics, and the geometry of the experimental facility was as follows: 30 m long and 0.50 m wide with vertical side walls. The channel was filled with a 0.20 m thick layer of sand with median grain size $d_{50} = 160\ m\mu$. The average velocity was 0.51 ms^{-1} and the water depth was approximately equal to 0.39 m at the channel inlet. The experiment considered in this work involved a trench with side slope 1:3.

To mimic the laboratory conditions with the model, a constant water depth of 0.3775 m above the bottom of the flume was imposed at the downstream outlet, and a constant discharge of 0.09945 $m^2 s^{-1}$, was specified at the upstream inlet. Flow and suspended sediment transport were computed with a fixed bed until steady flow conditions were reached in order to initialize the sediment and flow velocity, and with a movable bed afterwards in which the trench propagates in the direction of the flow. For this configuration, the flow decelerates by keeping the cross-trench water flux constant, resulting in the deposit of the upstream portion, where the

bottom profile tends to be linear and the erosion of the downstream portion, where the disturbance is travelling downstream.

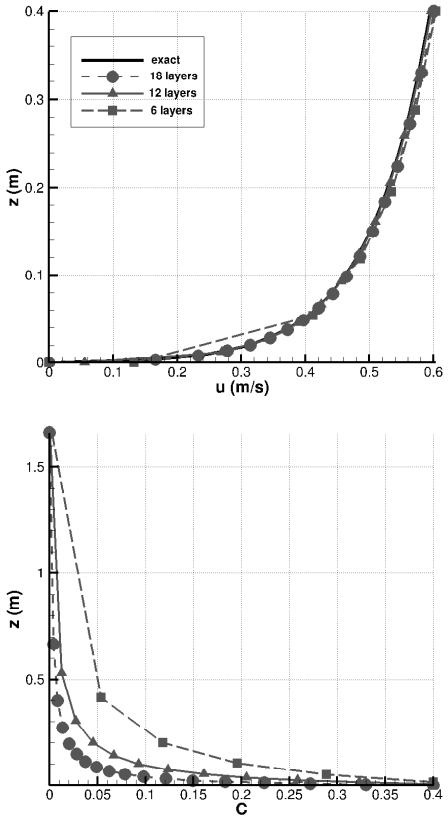

Figure 2. Velocity (left) and concentration profiles (right) for 6, 12 and 18 layers at channel outlet.

The modelled channel was represented using a mesh of 68,210 elements. For this model, 20 vertical layers were used, a thickness of the top layer of about 0.05 *m* and the thickness of the bottom layer equals of about 0.005 *m*.

The steady-state measured and computed velocity and sediment concentration profiles at five sections corresponding to 7 *m*, 9 *m*, 10.5 *m*, 12.75 *m* and 14 *m* from the channel inlet at the centreline of the flume are shown in Figures 3 and 4. In all figures, the circles correspond to experimental data.

Figures 3 and 4 show the velocity and suspended sediment concentration profiles at steady-state, obtained with the near-bed reference concentration approaches of van Rijn and Zyserman and Fredsoe using the mixing-length turbulence model. As showed, the velocity profiles are well captured by both approaches while van Rijn approach captures better the concentration profiles than the Zyserman and Fredsoe formula.

Results of the migration of the trench after 15 hours are showed in Figure 5. The computations are performed with the reference concentration of van Rijn and the mixing-length turbulence model. For the adopted configuration the results obtained with both models match the measurements of velocity, although some discrepancies are observed for the suspended sediment profiles. A detail of the bed level profile at $t = 0$ and $t = 15$ hours is showed in Figure 5. For the "classical" and "corrected" 2D model, the migrated distance of the trench is captured well but the trench filling is much too large in comparison with observations. Nevertheless, some little improvement is observed when the velocity correction terms are included [7]. The discrepancies between 2D simulations and observed data could be associated to the fact that the shallow water hypothesis are no longer valid for this channel configuration. The 3D model captures very well the migrated distance of the trench and the bed level profile is in good agreement with the observed data.

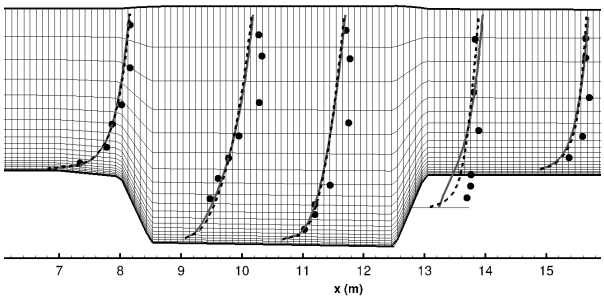

Figure 3. Velocity profiles computed with different c_{ref} and z_{ref}. Circles: experimental data of van Rijn [12]; solid: sediment closure formula of van Rijn; dashed: sediment closure formula of Zyserman and Fredsoe.

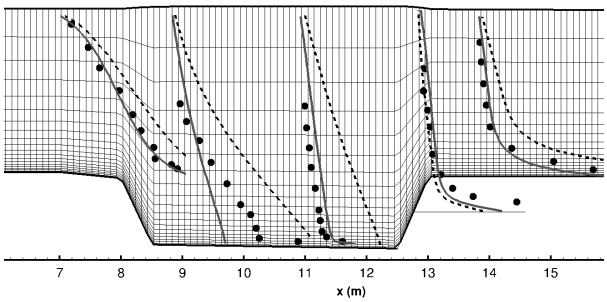

Figure 4. Concentration profiles computed with different c_{ref} and z_{ref}. Circles: experimental data of van Rijn [12]; solid: sediment closure formula of van Rijn; dashed: sediment closure formula of Zyserman and Fredsoe.

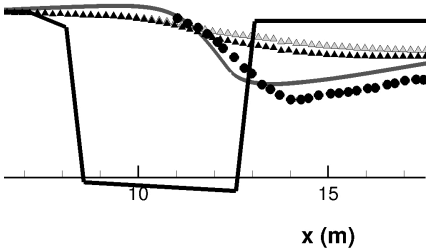

Figure 5. Detail of the migrating trench. Circles: experimental data of van Rijn [12]; Black solid: initial configuration; Grey solid: 3D simulations after 15 hours; Grey triangle: "classical"' 2D simulation after 15 hours; Black triangle: "corrected" 2D simulation after 15 hours.

V. CONCLUSIONS

In this paper, a 3D model for the flow, suspended sediment transport and bed evolution has been presented and compared with 2D simulations and experimental data. The model, implemented on the basis of the open-source, finite element/finite volume Telemac Modelling System, showed good agreement when compared against analytical and laboratory measurements of velocity and suspended sediment profiles. Furthermore, the simulations yielded successful predictions of the bed evolution.

The 2D simulations were performed with the "classical" shallow water equations and a "corrected" formulation that takes into account the fact that the largest part of the sediment is transported near the bed [7]. As expected, the classical 2D approach fails to reproduce accurately the observed data. The corrected approach introduces some improvements in the solution but the trench filling is still much too large in comparison with observations. The 3D model captures very well the migrated distance of the trench and the bed level profile is in good agreement with the observed data after 15 hours. The results are also in agreement with simulations of Lesser *et al.* [8] and Warner *et al.* [14].

Future work will examine on one hand the ability of the model to reproduce complex 3D flow structures, such as helicoidal flows in curved channels, on the other hand the coupling of the suspended transport with bed-load transport and the modelling of variable-size sediment.

REFERENCES

[1] Amoudry L.O. and Souza A., 2011. Impact of sediment-induced stratification and turbulence closure on sediment transport and morphological modelling. *Continental Shelf Research*, 31, 912-928.

[2] Begnudelli L., Valiani A. and Sanders B.F., 2010. A balanced treatment of secondary currents, turbulence and dispersion in a depth-integrated hydrodynamic and bed deformation model for channel bends. *Advances in Water Resources*, 33(1).

[3] Burchard H. (2002) *Applied Turbulence Modelling in Marine Waters*. Lecture Notes in Earth Sciences. Springer.

[4] Cao Z. and Carling P.A. (2002) Mathematical modelling of alluvial rivers: reality and myth. Part I:General review. *Proc. Inst. Civil Eng., Water & Maritime Eng*. 154(3).

[5] Celik I. And Rodi W. (1988). Modeling suspended sediment transport in non equilibrium situations, *Journal of Hydraulic Engineering*, vol. 114 (10), pp 1157-1188.

[6] Hervouet J.-M. (2007) Hydrodynamics of Free Surface Flows. Modelling with the finite element method. John Wiley & Sons, Ltd.

[7] Huybrechts N., Villaret C. and Hervouet J.-M. (2010) Comparison between 2D and 3D modelling of sediment transport: application to the dune evolution. *Proc. River Flow Conf.*, Germany.

[8] Lesser G.R., Roelvink J.A., van Kester J.A.T.M and Stelling G.S. (2004) Development and validation of a three-dimensional morphological model. *Coastal Engineering*, 51 883-915.

[9] Nezu, I. and Nakagawa, H. (1993) *Turbulence in Open-Channel Flows*, IAHR Monograph, Rotterdam, The Netherlands.

[10] Rodi, W. (1993) *Turbulence Models and Their Applications in Hydraulics*, 3rd ed., IAHR Monograph, Rotterdam, The Netherlands.

[11] Telemac Modelling System (2011) http://www.opentelemac.org /

[12] van Rijn L.C. (1987) Mathematical modelling of morphological processes in the case of suspended sediment transport. Delft Technical University, The Netherlands.

[13] Vreugdenhil C. (1994) *Numerical methods for shallow-water flow*, Kluwer Academic Publishers.

[14] Warner J.C., Sherwood C.R., Signell R.P., Harris C. and Arango H.G. (2008) Development of a three-dimensional, regional, coupled wave, current, and sediment-transport model. *Computers and Geosciences* 34, 1284-1306.

[15] Wu, W. (2008) *Computational River Dynamics*. Taylor and Francis Group, London, UK.

[16] Zeng J., Constantinescu G. and Weber L. (2008) A 3D non-hydrostatic model to predict flow and sediment transport in loose-bed channel bends. *J. Hydr. Research*, 46: 3, 356-372.

[17] Zyserman J. and Fredsoe J. (1994) Data Analysis of Bed Concentration of Suspended Sediment, *J. Hydr. Eng.*, 120(19), 1021-1042.